Journal of Southeast University (English Edition) Vol. 28, No. 2, pp. 184 - 189 June 2012 ISSN 1003—7985

Main properties of ultra-high performance fiber reinforced cement composites under couple effect of load and environment

Saly Fathy[1,2] Gu Chunping[1] Sun Wei[1]

([1] School of Materials Science and Engineering, Southeast University, Nanjing 211189, China)
([2] Department of Civil Engineering, Alexandria University, Alexandria 21532, Egypt)

Abstract: This study aims to reveal the mechanism that how the content of steel fibers and strength grades affect the macro performance of the ultra-high performance fiber reinforced cementitious composite (UHPFRCC) and to study the UHPFRCC durability under the combined effect of loads and environments. Three types of high and ultra-high performance fiber reinforced cement composites with different strength grades (100, 150, 200 MPa) and different steel fiber volume fractions (0%, 1%, 2%, 3%) are prepared. The main properties of mechanical performance and short-term durability are studied. A preloading frame is designed to apply a four-point load external flexural stress with a stress selection ratio of 0.5 for UHPFRCC150 specimens. The results show that the growth in strength grade with a proper content of steel fiber greatly increases the strength and toughness of the HPFRCC and the UHPFRCC while decreasing the dry-shrinkage ratio. For the loaded specimens, the existence of steel fiber can reduce the negative influence of tensile stress on the Cl^- penetration resistance of the UHPFRCC in addition to improving its ability to resist the freeze-thaw damage.

Key words: ultra-high performance fiber reinforced cementitious composite; couple effect of load and environment; mechanical properties; durability

doi: 10.3969/j.issn.1003-7985.2012.02.010

The development of mechanical properties is fundamental for the design and construction of cement based material structures[1]. Ultra-high performance cementitious composites (UHPCC), developed in France approximately two decades ago, are a relatively new class of concrete that has superior performance characteristics compared with the conventional concrete. The improved strength and durability properties of UHPFRC are mainly due to the optimized particle gradation that produces a very tightly packed mixed density, the use of steel fibers, and an extremely low water to binder ratio[2].

On the real conditions of concrete, durability and load conditions have a very close relationship, but they only consider the role of a single factor, which may overstate the true durability of concrete structures. The coupled effect of loads and environments must be considered for improving the reliability and accuracy of the concrete study [3]. As a result, Refs. [3-6] gradually realized the urgent need to focus on the coupling effect of loads and environments on cement-based materials. Therefore, this paper presents the results of an experimental study on the main properties of high and ultra-high performance fiber reinforced cementitious composites under different strength grades (100, 150, 200 MPa) and different steel fiber volume fractions (0%, 1%, 2%, 3%) with or without the effect of loads. Specimens are cured in standard conditions ((20±2) ℃, RH>95%) for 90 d.

1 Experimental

1.1 Materials

The high early strength Portland cement (PC) used in the experiments is produced by Jiangnan Cement Co., Ltd, Nanjing and it is classified as P·Ⅱ 52.5R according to the Chinese standards. The physical and mechanical properties of the materials are shown in Tab. 1. Grade Ⅰ fly ash (FA), similar to Class F fly ash according to the ASTM, is supplied by Zhenjiang Power Plant with a specific surface area of 454 m^2/kg. Silica fume (SF) used in the experiments is produced by the Ai Ken Company with a specific surface area of 22 000 m^2/kg. The oxide compositions of the PC, FA and SF analyzed with the X-Ray fluorescence spectroscopy are listed in Tab. 2.

Ordinary river-sand with a maximum diameter of 2.36 mm, a fineness module of 2.44, and a packing and apparent density of 1.4 and 2.4 g/cm^3, respectively, is used as a fine aggregate. A visconcrete 3301 superplasticizer supplied by Switzerland Sika (China) Building Materials Co., Ltd. with a water reducing ratio of more than 30% and a solid content of 28% is used. Dramix, a superfine steel fiber covered by copper is incorporated. The fibers are 13 mm long and have a circular cross-section with a diameter of 0.2 mm.

Received 2012-01-06.

Biographies: Saly Fathy (1985—), female, graduate; Sun Wei (corresponding author), female, professor, academician of China Engineering Academy, sunwei@seu.edu.cn.

Foundation items: The Technical Research Program from NV Bekaert SA of Belgium (No. 8612000003), the National Natural Science Foundation of China (No. 50908047).

Citation: Saly Fathy, Gu Chunping, Sun Wei. Main properties of ultra-high performance fiber reinforced cement composites under couple effect of load and environment[J]. Journal of Southeast University (English Edition), 2012, 28(2): 184 - 189. [doi: 10.3969/j.issn.1003-7985.2012.02.010]

Tab. 1 Physical and mechanical properties of cement

Standard consistency/%	Initial setting time/min	Final setting time/min	Flexural strength/MPa		Compressive strength/MPa		Specific surface area/($m^2 \cdot kg^{-1}$)
			3 d	28 d	3 d	28 d	
26.3	140	245	7.2	10.6	34.7	62.8	362

Tab. 2 Oxide compositions of the FA and SF %

Mineral admixture	$w(SiO_2)$	$w(Al_2O_3)$	$w(Fe_2O_3)$	$w(CaO)$	$w(MgO)$	$w(SO_3)$	$w(K_2O)$	$w(Na_2O)$	Loss
FA	54.88	26.86	6.49	4.77	1.31	1.16	1.05	0.88	2.5
SF	94.48	0.27	0.83	0.54	0.97	0.8			2.13

1.2 Mix proportion

All of the bases highlighted in the international definitions and discussed above are utilized for the design of the cementitious materials with three different strength grades: HPFRCC100, UHPFRCC150 and UHPFRCC200. In addition, different volume fractions of steel fibers are added into the control matrix of UHPFRCC150 to reveal the influence of the amount of steel fiber on the mechanical properties and durability of the UHPFRCC. Three mixture proportions of the cement composites are designed in the experiment, of which the sand-to-binder ratio (S/B) and the super plasticizer content (SP) is constant. φ_{SF} is the volume fraction of steel fiber. The composition of cementitious materials is a total of 100%. The proportioning of the concrete mixture is listed in Tab. 3.

Tab. 3 Mixture proportions in the present study %

Strength grade	w_C	w_{FA}	w_{SF}	S/B	w_{SP}	W/B	φ_{SF}
HPFRCC100	50	50	5	120	3.5	0.17	1
UHPFRCC150	50	40	10	120	3.5	0.16	2
UHPFRCC200	50	35	15	120	3.5	0.15	3
UHPFRCC150(0%)	50	40	10	120	3.5	0.16	0
UHPFRCC150(1%)	50	40	10	120	3.5	0.16	1
UHPFRCC150(3%)	50	40	10	120	3.5	0.16	3

1.3 Specimen preparation

The main aspect in specimen preparation is to produce uniform distribution of UHPFRCC components including binder materials and steel fibers. Therefore, according to the Chinese standard test method JTJ 270—98 and the mixture proportions in Tab. 3, fresh concrete mixtures are cast into steel molds to produce samples with a dimension of 40 mm × 40 mm × 160 mm, and then placed on a shaking table in order to achieve good compaction. After the samples are kept for 24 h at room temperature, the prism specimens are demoulded and cured for standard curing at a temperature of (20 ± 2) ℃, with a relative humidity RH > 95%.

1.4 Test method

1.4.1 Mechanical properties test method

According to the Chinese standard GB/T 50081—2002, the bending specimen size is a prism (40 mm × 40 mm × 160 mm). Applying a three-point bending test, the span is 100 mm, and the loading rate is 1 mm/min. The compressive strength specimen is a 40 mm × 40 mm × 40 mm cube.

1.4.2 Durability test method

In this study, a spring type of the preloading frame is prepared to apply a four-point load external flexural stress with a 135 mm span to the specimens, as shown in Fig. 1. The frame is made up of stainless steel, and the applied load that comes from the elastic forces of spring compression is shown in Fig. 2[4]. The selection ratio of the flexural load stress in the test (i.e., the ratio of externally applied flexural load to the ultimate flexural load capacity) in this study is 0.5, which is applied to the specimens by screwing in a bolt, and controlled by the compression length.

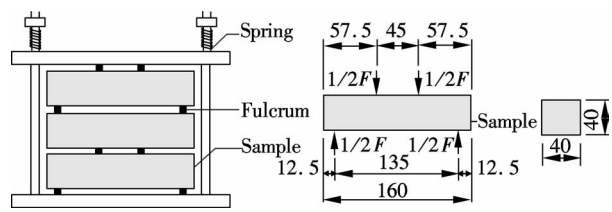

Fig. 1 Schematic for UHPFRCC pre-loading(unit: mm)

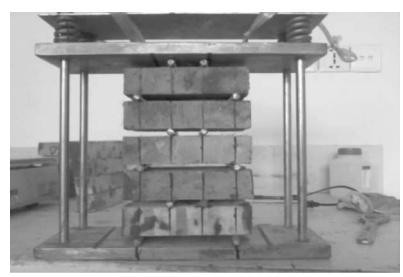

Fig. 2 The loading device

According to the Chinese standard GB/T 50082—2009, after curing 3 d, specimens are placed in a chamber at a constant temperature of (20 ± 2) ℃ and a humidity of (60 ± 5)%. Immediately after the removal of the specimens from the curing room to the test lab at room temperature, the initial lengths are measured. The deformation measurements are procured according to the following curing time: 1, 3, 7, 14, 28, 45, 60, 120, 150, 180 d.

The freeze-thaw test is also according to GB/T 50082—2009. The test data are collected once after every 25 freeze-thaw cycles to determine the weight-loss rate and the relative dynamic elastic modules of the specimens.

In this study, the chloride analysis is undertaken according to the Chinese standard JTJ 270—98 and the NT

Build 443—95[7] titration. After taking the specimens from curing rooms, each specimen is coated with gas-tight epoxy resin. One surface of each specimen is left uncoated for the purpose of exposing this surface to a NaCl solution[5]. The preloading concrete specimens are placed together with the loading frame into a chloride solution, NaCl with a 10% mass fraction for 2, 3, 4 months, respectively. Immediately after the specified immersion period, the pre-loading frame is removed, and the specimens are taken out and dried for 2 d at (60 ± 3) ℃. Powder specimens are collected from finite depths: 0 to 5 mm, 5 to 10 mm, 10 to 15 mm and 15 to 20 mm. At each depth, two samples are taken. One sample is extracted from the tension surface, the other from the compression surface. Using a drill, at least 5 g of fine powder is extracted from each cementitious composite layer. Subsequently, the chloride content, as a percentage of Cl^- by the mass of concrete is determined.

2 Results and Discussion

2.1 Mechanical properties

2.1.1 Effect of strength grade on the mechanical properties of HPFRCC and UHPFRCC

The data in Tab. 4 represent the flexural and compressive strength of UHPFRCC100, UHPFRCC150 and UHPFRCC200 after 90 d of standard curing. From this data, it can be concluded that the strength increases with the increase in silica fume and steel fiber content and the decrease in the water/binder ratio. Furthermore, the strength values after standard curing for 90 d are to meet the design requirements. For example, the compressive strength of C200 increases by 70% and the flexural strength by 106% in contrast to the smaller values of C100 at the same curing age. At the crack tip, steel fibers can restrain the extension of the crack and reduce the extent of stress concentration at the tip of a crack, thus changing the direction of crack growth and delaying the growth rate of a crack[6]. However, silica fume increases the interfacial characteristics due to its filler effect, crystallizing effect, and pozzolanic effect.

Tab. 4 Strength of HPFRCC and UHPFRCC after 90 d standard curing

Strength grade	Flexural strength/MPa	Compressive strength/MPa
HPFRCC100	19.6	124.9
UHPFRCC150	38.6	156.1
UHPFRCC200	40.5	212.7

2.1.2 Effect of volume fraction of steel fiber on the mechanical properties of UHPFRCC

In this study, steel fibers with different volume fractions (0%, 1%, 2% and 3%) are added to the UHPFRCC150 matrix in order to understand the enhanced role of the steel fibers. Compressive and flexural strength results of different fiber contents after 90 d standard curing are shown in Fig. 3. It can be seen from Fig. 3 that the compressive and flexural strength increases with the increase in UHPFRCC fiber content. The increase of flexural strength is particularly sensitive to the fiber volume fraction. The incorporation of 1% steel fiber into a cement matrix is not very effective for strength as it incorporates 2% and 3 % steel fiber. Adding 2% steel fiber to UHPFRCC specimens increases the flexural strength two times more than those without steel fiber. In addition, adding 3% steel fibers makes the flexural strength reach 2.7 times its value without fibers. This is due to the bridging effect of the fiber which is responsible for carrying loads after the appearance of cracks[8]. Furthermore, increasing the volume fraction of steel fiber in UHPFRCC150 leads to an increase in the energy absorbed by its matrix. As illustrated in Fig. 4, specimens without fibers reach ultimate flexural strength after brittle fracture. Conversely, the incorporation of 1% steel fibers not only increases the strength of UHPFRCC but also increases the area under the load deflection curve, significantly enhancing the fracture toughness and thus preventing sudden failure.

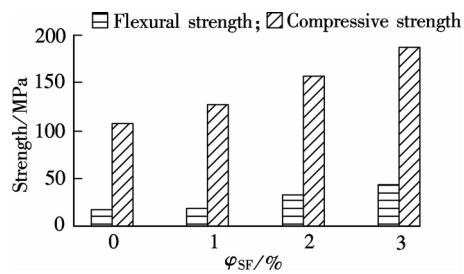

Fig. 3 Flexural and compressive strength of UHPFRCC150 with different steel fiber volume fractions after 90 d of curing

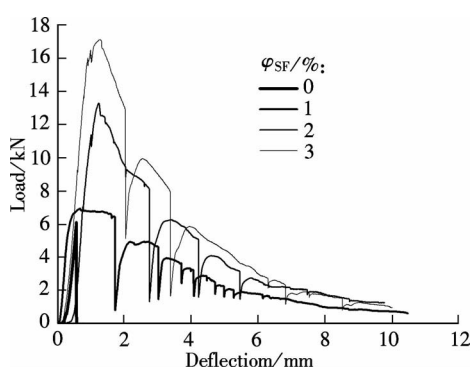

Fig. 4 Load-deflection curve of UHPFRCC with different steel fiber volume fractions

2.2 Results of durability test

2.2.1 Shrinkage test results

Fig. 5 shows the shrinkage strain resulting from drying the shrinkage measurements of high and ultra-high performance fiber reinforced cementitious composites. The shrinkage strain of UHPFRCC for 180 d is limited to 400 $\times 10^{-6}$ and 600 $\times 10^{-6}$ which is slightly less than ordinary concrete values (500 $\times 10^{-6}$ to 900 $\times 10^{-6}$) [9]. Due to

the low water/cement ratio and the incorporation of a high amount of mineral admixtures in UHPFRCC matrix, the permeability and the number of pores is greatly reduced. Therefore, the rate of the drying shrinkage is reduced, since it will take more time for the water to find its way out of the specimen. In addition, as can be seen from Fig. 5, the shrinkage strain is reduced with the increase in the volume fraction of steel fiber[10]. The shrinkage strain is reduced with the increase in the steel fiber from 0% to 3%, respectively.

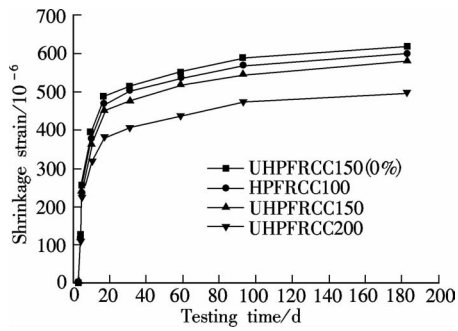

Fig. 5 Shrinkage strain of HPFRCC and UHPFRCC at different testing times

2.2.2 Cl^- concentration in UHPFRCC150 after different immersion time

Fig. 6 shows the Cl^- concentration distribution at different depths of unloaded immersed UHPFRCC150 in 10% NaCl at 2, 3 and 4 months, respectively. It can be concluded that Cl^- diffusion concentration increases at a lengthier immersion time. The chloride concentration values for 2 and 3 months immersion at different depths are very close, but it increases slightly after four months of immersion, indicating that Cl^- penetrates very slowly into UHPFRCC. This is mainly due to its low porosity and dense microstructure.

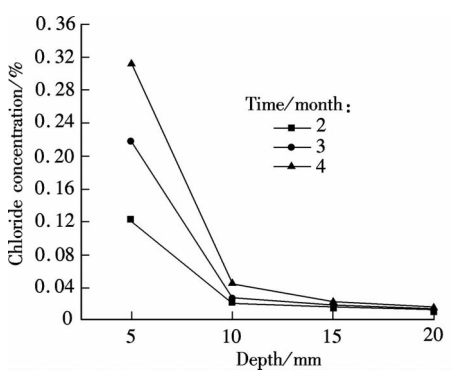

Fig. 6 Chloride concentration at different depths of UHPFRCC150 after different immersion times

2.2.3 Resistance of different HPFRCC and UHPFRCC strength to Cl^- diffusion

Fig. 7 shows the free Cl^- concentration distribution at different depths of different HPFRCC and UHPFRCC soaked for three months. The figure shows that the free Cl^- concentration values for HPFRCC100 and UHPFRCC150 are very close, but the free Cl^- concentration in UHPFRCC200 is about 50% lower. This is mainly because UHPFRCC200 has the lowest w/c ratio (0.15) and the highest silica fume percentage (15%) of the three intensity levels.

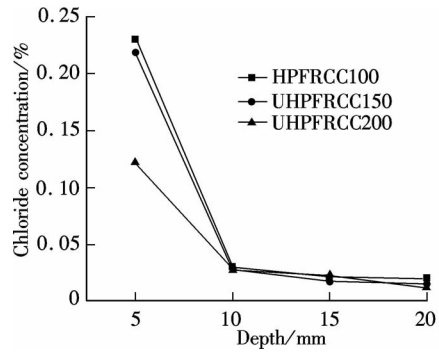

Fig. 7 Chloride concentration at different depths of different HPFRCC and UHPFRCC after 90 d immersion

2.2.4 Effect of loading and φ_{SF} on the UHPFRCC resistance to Cl^- penetration

Figs. 8 and 9 show the results of the chloride concentrations at different depths of UHPFRCC150 (0%) and UHPFRCC150 (2%), respectively, at different stress states after a three-month immersion. As it can be concluded from the two figures that the resistance to Cl^- penetration for the tension side is less than that in non-loaded specimens while the higher resistance to Cl^- penetration is on the side of compression. The effect of adding steel fibers

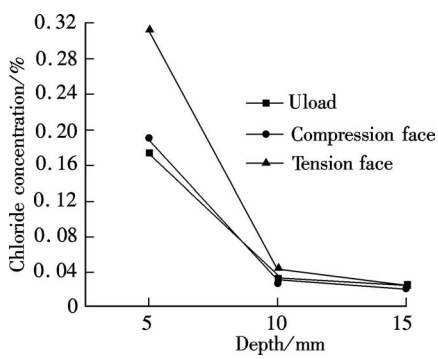

Fig. 8 Chloride concentration at different depths of UHPFRCC150 (0%) with different stress states after 90 d immersion

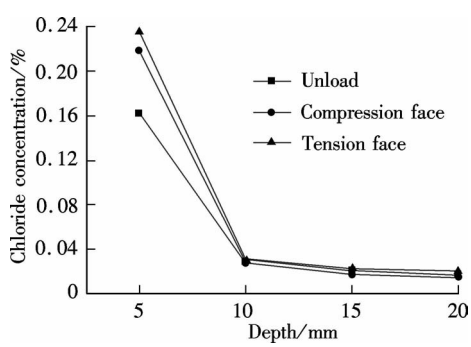

Fig. 9 Chloride concentration at different depths of UHPFRCC150 with different stress states after 90 d immersion

implied by the unloaded UHPFRCC150 ($\varphi_{SF}=2\%$) and UHPFRCC150 (0%) chloride concentration at 0 to 5 mm depth is about 0.22 and 0.2, respectively.

2.2.5 Effect of loading and strength grade on frost resistance of HPFRCC and UHPFRCC

Figs. 10 and 11 show an extremely excellent anti-freeze-thaw performance of all the specimens. After 800 cycles of freezing and thawing, damage does not occur. The weight loss rate is very slow and mostly concentrated in about 0.5%. Only the weight loss rate of loaded UHPFRCC150 (725 cycles) is relatively high, reaching 1.0%. At the beginning of freeze-thaw cycles, contrary to what is expected, we observe some increase in the specimen weight. The pores in UHPFRCC expand under the frost effect, resulting in water absorption increasing and a slight increase in the weight of the specimen. By continuing freeze-thaw cycles, the specimen gradually peels and spalls; therefore, the weight loss successively increases[11].

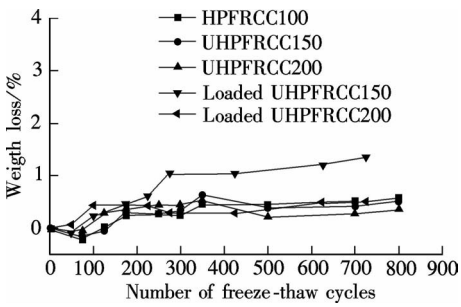

Fig. 10 Effect of strength and load on weight loss of HPFRCC and UHPFRCC

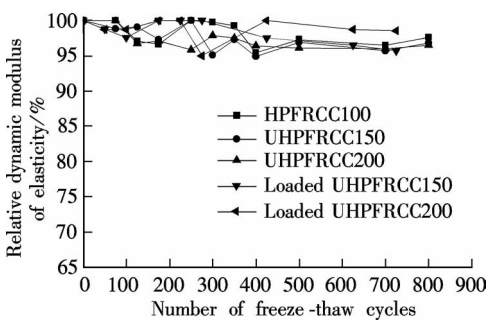

Fig. 11 Effect of strength and load on relative dynamic modulus of elasticity of HPFRCC and UHPFRCC

Under the action of freeze-thaw cycles, a large number of micro-cracks appears and the internal structure of the matrix loosens. All these factors lead to the increase in the relative dynamic elastic modulus of different strength grades for HPFRCC and UHPFRCC as shown in Fig. 11. After 800 cycles the relative dynamic elastic modulus reduction for both the loaded and the unloaded specimens is only 5% for all strength levels. This value is very low due to a low *w/c* ratio and high proportion of silica fume thus improving the internal pore structure.

The weight loss of UHPFRCC increasing and the relative dynamic elastic modulus decreasing in the loaded cases are more than those in the non-loaded cases, because the static load stress results in the increase in the number of cracks, and coupled with freeze-thaw cycles, the crack expansion is increased, leading to material failure.

2.2.6 Effect of steel fiber volume fraction on UHPFRCC frost resistance

Figs. 12 and 13 reveals the effect of the volume fraction of the fiber on weight loss and the relative dynamic elastic modulus of UHPFRCC. After 800 cycles of freezing and thawing, the weight loss of UHPFRCC150 increases about 0.5%. Similarly, as the relative dynamic elastic modulus increases, so does the steel fiber volume fraction. Thus, due to the inhibitive bridging effect of fibers on crack propagation, the matrix has a decreasing rate of surface spall. Conversely, the weight loss and the relative dynamic elastic modulus values for UHPFRCC150 (0%) are more than 1.0% and 90%, respectively. The cracks caused by freeze-thaw cycles are not controlled as a result of the absence of fibers. This leads to an increasingly deteriorated matrix.

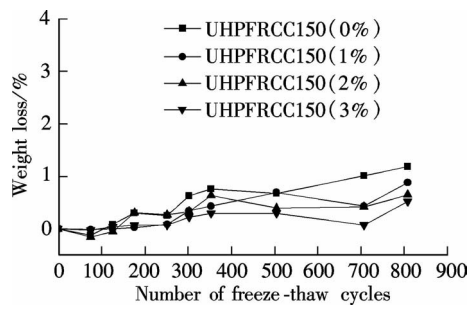

Fig. 12 Effect of the volume fraction of steel fiber VF on mass loss of UHPFRCC

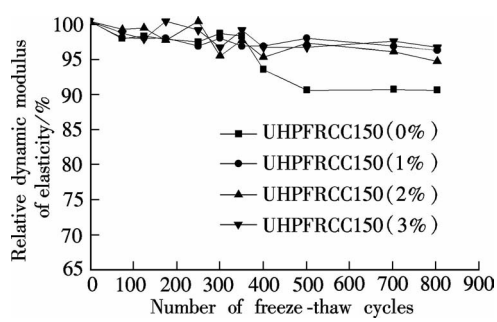

Fig. 13 Effect of the volume fraction of steel fiber on relative dynamic modulus of elasticity of UHPFRCC

3 Conclusion

This research presents an alternative to the use of high temperature curing in the production of UHPFRC pre-cast elements. In addition, the results point to the possibility of using standard curing ((20 ± 2) ℃, RH > 95%) for 90 d while successfully meeting strength requirements and maintaining high mechanical performance at all three distinct strength levels of high and ultra-high performance fiber reinforced cement composites. The different propor-

tions used in this study show excellent short-term durability of shrinkage strain, resistance to Cl^- penetration and frost resistance even for specimens subjected to the coupled effect of static load and environment. After 800 freeze-thaw cycles, the weight loss and the relative dynamic elastic modules are only about 5% and 95%, respectively. Furthermore, the incorporation of steel fiber prevents the sudden brittle failure of the matrix under flexural loads. In the absence of loading, steel fibers have a slight effect on UHPFRCC resistance to Cl^- penetration. However, under the effect of static loading, the presence of fibers perform well at suppressing the formation and the expansion of micro-cracks, thus greatly enhancing the resistance of the matrix to Cl^- penetration and proving the urgency of adding steel fibers in the production of UHPFRCC.

References

[1] Katrin H, Marco V. Development of the mechanical properties of an ultra-high performance fiber reinforced concrete (UHPFRC) [J]. *Cement and Concrete Research*, 2006, **36**(7): 1362 - 1370.

[2] Maher K T, George M. Application of ultra-high performance concrete to bridge girders. NDOR: P310[R]. Lincoln: Nebraska Department of Roads (NDOR), 2009.

[3] Sun Wei. New research and application progress of high performance concrete in China [R]. Nanjing, China: Southeast University, 2010.

[4] Zhang Yunsheng, Sun Wei, Chen Shudong, et al.. 1D and 2D carbonation of fly ash concrete under flexural stress [J]. *Journal of Southeast University*: *Natural Science Edition*, 2007, **37**(1): 118 - 122. (in Chinese)

[5] Zhang Yunsheng, Sun Wei, Chen Shudong, et al. One and two dimensional chloride ion diffusion of fly ash concrete under flexural stress [J]. *Journal of Zhejiang University*: *Science A*, 2011, **12**(9): 692 - 701.

[6] Diao Bo, Sun Yang, Cheng Shaohong, et al. Effects of mixed corrosion, freeze-thaw cycles, and persistent loads on behavior of reinforced concrete beams [J]. *Journal of Cold Regions Engineering*, 2010, **25**(1): 37 - 52.

[7] Nordtest method. Concrete, hardened: accelerated chloride penetration. NT Build 443 [R]. Espoo, Finland: Nordtest, 1995.

[8] Li V C, Strang H, Krenchel H. Micromechanics of crack bridging in fiber-reinforced concrete [J]. *Materials and Structures*, 1993, **26**(8): 486 - 494.

[9] Yan Handong, Sun Wei, Chen Huisu. The effect of silica fume and steel fiber on dynamic mechanical performance of high-strength concrete [J]. *Cement and Concrete Research*, 1999, **29**(3): 423 - 426.

[10] Sun Wei, Chen Huisu, Luo Xin, et al. The effect of hybrid fibers and expansive agent on the shrinkage and permeability of high-performance concrete [J]. *Cement and Concrete Research*, 2001, **31**(4): 595 - 601.

[11] Behfarnia K. Studying the effect of freeze and thaw cycles on bond strength of concrete repair materials [J]. *Asian Journal of Civil Engineering* (*Building and Housing*), 2010, **11**(2): 165 - 172.

荷载与环境因素耦合作用下超高性能水泥基复合材料的主要性能

Saly Fathy[1,2]　顾春平[1]　孙　伟[1]

([1] 东南大学材料科学与工程学院,南京 211189)

([2]Department of Civil Engineering, Alexandria University, Alexandria 21532, Egypt)

摘要:研究了钢纤维掺量和强度等级对超高性能纤维增强水泥基复合材料(UHPFRCC)宏观性能的影响及UHPFRCC在荷载与环境因素耦合作用下的耐久性能. 制备了3组不同强度等级(100, 150, 200 MPa)和不同纤维掺量(0%, 1%, 2%, 3%)的高与超高性能水泥基复合材料,并且测试了其各项力学性能和短期耐久性能. 利用设计的预加载装置,在UHPFRCC150试件上施加了应力比为0.5的四点弯曲荷载. 结果表明,随着强度等级的增加,在掺加适量钢纤维掺量的情况下,高与超高性能水泥基复合材料的强度和韧性均明显提高,同时其干燥收缩值降低. 对于加载的试件,钢纤维降低了拉应力对UHPFRCC抗氯离子渗透性能的不利影响,并且提高了材料的抗冻融性能.

关键词:超高性能纤维增强水泥基复合材料;荷载与环境耦合作用;力学性能;耐久性

中图分类号:TU528